P2.8 ASSIMILATION OF SURFACE OBSERVATIONS IN COMPLEX TERRAIN

Xingxiu Deng* and Roland B. Stull
University of British Columbia,
Vancouver, BC, Canada

ABSTRACT

Built upon the recent success of objective analyses of potential temperatures in complex terrain using a mother-daughter approach, experiments are conducted to evaluate the impacts of assimilating surface temperatures on subsequent forecasts. The mother-daughter approach spreads surface valley observations along circuitous valleys in complex terrain, while reducing spread over mountain ridges.

This approach is further refined for mountain-top observations in this study, to allow spreading the mountain-top observations to neighboring high ridges across valleys. This study also demonstrates how to combine detailed surface analyses from local observations with coarse-resolution analyses from major operational centers, such as the Eta analysis from the National Centers for Environmental Prediction (NCEP). Incremental analysis update (IAU) is used to incorporate the final analysis increments into a mesoscale numerical weather prediction model. To assess the impacts on mesoscale forecasts of surface data assimilation, assimilation runs started from the combined analyses are compared with control runs driven by unmodified Eta initial conditions. It is found that the model improves surface temperature and mean sea level pressure forecasts during the first 12 h forecast period after assimilating surface temperatures.

1. INTRODUCTION

Nowadays, people tend to rely heavily on numerical weather prediction (NWP) forecasts beyond the first few hours. The rapid growing computer power has led to finer resolution NWP models, which are able to resolve mesoscale features and thus to give more accurate forecasts. This capability is of utmost importance for mountainous British Columbia (BC) because valleys are mesoscale, and most of the population and commence is in such valleys. However, accurate high-resolution forecasts depend on accurate and representative initial fields from which to start.

Determining the best initial conditions for NWP models is the purpose of data assimilation (DA). There exists many methods for this purpose, such as successive correction methods, statistical (or optimum) interpolation, Kalman filtering, and variational methods (Daley 1991, Kalnay 2003).

Surface observations, being frequent and dense, are valuable data sources for mesoscale data assimilation and forecasting (Miller and Benjamin 1992, Ruggiero et al. 1996). For example, it was found that assimilating surface data into NWP models significantly reduced modeling errors in the atmospheric boundary layer (Alapaty et al. 2001), which might be useful for subsequent air pollution modeling. However, assimilating surface observations into NWP models still remains a relatively unexplored area for improving the initial conditions of NWP models, particularly in complex terrain; i.e., British Columbia, Canada.

A mother-daughter (MD) approach was developed for the objective analysis of surface observations in complex terrain (Deng and Stull 2004). The approach generates sharing factors (SFs) and circuitous travel distance (CTD), which are then used to define anisotropic correlation function for the ADAS Bratseth scheme (Brewster 1996, Bratseth 1986). This allows observation information to follow valleys around ridges, while reducing spread over the ridge top. This study further refines the MD approach by treating mountain-top observations differently than valley observations, and focuses on assimilating surface temperature observations in complex terrain into a NWP model. The main objective is to improve the forecast quality of surface fields.

2. MOUNTAIN-TOP REFINEMENT

Surface observation stations are usually located in valleys. But, there are some surface stations located at high elevations in mountains, such as at ski areas. The original MD approach in Deng and Stull (2004) is good for surface observations in valleys, but is problematic for mountain-top observations. The original MD approach is not able to spread information from a mountain-top observation to the grid points (GPs) of surrounding mountains. This is particularly true if the observation is located at the top of a very steep mountain. The spreading to the surrounding mountain tops is desired for two reasons. During shallow cold-air pooling events, the high-mountain tops are all penetrating into the free atmo-

* *Corresponding author address:* Xingxiu Deng, Dept. of Earth & Ocean Sciences, University of British Columbia, 6339 Stores Rd. Vancouver, BC, Canada V6T 1Z4. E-mail:xdeng@eos.ubc.ca

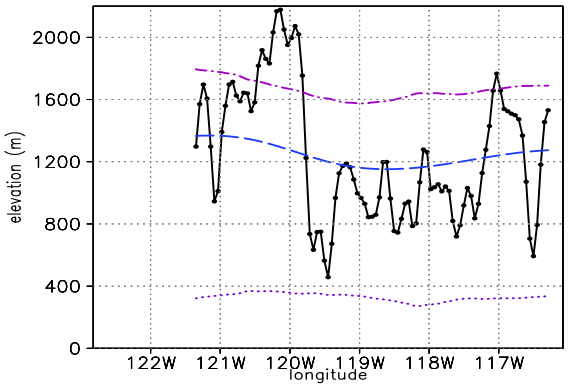

Figure 1: Cross section of the model topography (solid line), the smoothed model topography (dashed line), the approximated height of BL top (dot dashed line) and the standard deviation of the difference between the model topography and the smoothed model topography (dotted line). The cross section is along 49.0 °N in the domain shown in Fig. 2. Any observation located above the dot dashed line will be treated as a mountain-top observation.

sphere where they would experience the same weather. Second, during deep boundary layer (BL) events with BL top above the mountain top, vigorous turbulence would also cause mixing across the valleys. Therefore, the MD approach is further refined here to allow such spreading by treating mountain-top observations differently than valley observations.

Recall that the original MD approach is expressed by the following iterative equation for sharing factor S_{od}:

$$S_{od}(\nu+1) = S_{om}(\nu)\left\{1-\left[\frac{|Z_m(\nu)-Z_d(\nu+1)|}{zref1}\right]^a\right\} \left\{1-\left[\frac{|Z_o-Z_d(\nu+1)|}{zref2}\right]^b\right\} \quad (1)$$

for $|Z_m(\nu)-Z_d(\nu+1)| < zref1$ and $|Z_o-Z_d(\nu+1)| < zref2$, otherwise $S_{od}(\nu+1)=0$. The subscripts o, m, d represent an observation, a mother GP and a neighboring daughter GP, respectively. Z is elevation, ν is iteration counter. The terrain-following and level-top BL-depth parameters are $zref1$ and $zref2$, respectively. Parameters a and b control the analysis decorrelation rate.

The modified sharing factor (SF) for a mountain-top observation is proposed as follows:

$$S_{od}^{MT} = S_{om}^{MT}\left\{1-\left[\frac{|Z_o-Z_d|}{zref2}\right]^b\right\} \quad (2)$$

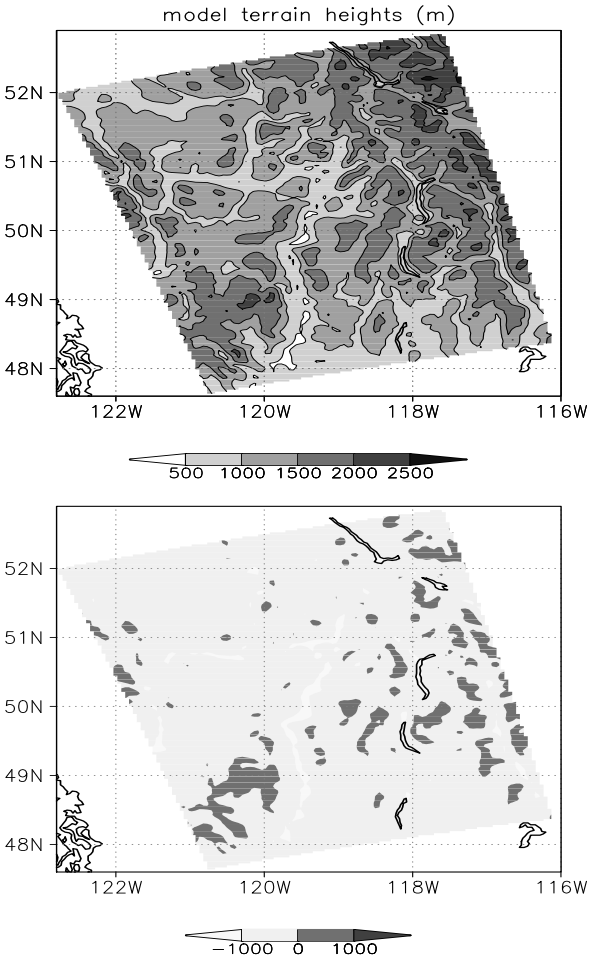

Figure 2: The model topography (up, darker shading indicates higher elevations) and the difference between the model topography and the approximated height of BL top (bottom, any station located in the darkly shaded areas will be treated as a mountain-top station).

for $|Z_o-Z_d| < zref2$, otherwise $S_{od}^{MT}=0$. The superscript MT indicates mountain-top observations. S_{om}^{MT} is the SF at the mountain-top observation location, which is 1.0. The SF at any surrounding GP depends upon the elevation difference between the observation and the GP and upon the level-top BL depth parameter $zref2$. No iteration is needed.

The refined MD approach first checks whether an observation is located at mountain-top or in a valley, and then picks the right equation to calculate the SF for that observation station. To distinguish mountain-top observations from valley observations, a simple approach is taken here. Firstly, the model topographic heights are smoothed by the Barnes (1964) method. The shape factor (R) of the empirical Gaussian weights is taken as 90 km, which is thirty times the grid-spacing (3 km). Secondly,

the standard deviation (σ_Z) of the difference between the model terrain height and the smoothed model terrain height is calculated within a region of (-*R*, +*R*). Let Z_s be the smoothed model terrain height, the long-term averaged height of BL top (Z_{BL}) is approximated by:

$$Z_{BL} = Z_s + max(0., zref2 - \sigma_Z) \quad (3)$$

where $zref2$ is the level-top BL-depth parameter in (1) and (2). The values of all parameters in (1) and (2) are the same as in Deng and Stull (2004): $a = 2$, $b = 2$, $zref1 = 750\ m$, $zref2 = 750\ m$. Fig. 1 is a cross section (along 49.0 °N in the domain shown in Fig. 2) of the model topography, the highly smoothed model topography (Z_s), the approximated height of BL top (Z_{BL}) and σ_Z. Any observation located above the Z_{BL} line will be treated as a mountain-top observation.

The model topography and the difference between the model topography and the approximated height of BL top are shown in Fig. 2 for our study domain centered at Vernon, British Columbia.

The approximation of Z_{BL} is crude, but provides a simple and effective way to distinguish mountain-top observations from valley observations. That is to compare the elevation of an observation with the approximated height of BL top (Z_{BL}). As mentioned in Deng and Stull (2004), in the case of an observation that is not co-located with any model GP, the station is first approximated as being co-located at whichever nearest neighboring model GP has the minimum elevation difference between them. In such a case, the elevation of the nearest neighboring model GP is compared with Z_{BL}. Any surface observation that is above Z_{BL} is treated as a mountain-top observation, whereas any surface observation that is below Z_{BL} is treated as a valley observation. The SF for a mountain-top observation is obtained through (2), whereas the SF for a valley observation is calculated via (1).

3. METHODOLOGY

Dense surface observations are valuable data sources for mesoscale data assimilation. However, surface observations are available only at one level. Meanwhile, major operational centers generate 3D meteorological analysis daily by assimilating many types of measurements. One example is the Eta model analysis from the National Centers for Environmental Prediction (NCEP). This study demonstrates how to effectively combine local surface data with 3D analysis from major operational centers.

Surface observations are first analyzed by using the refined MD approach in conjunction with the ADAS to generate a surface data analysis. This is done by optimumly combining surface observations and the first-guess at the lowest terrain-following level from the Mesoscale Compressible Community (MC2) model at 3 km grid-spacing. In this study, the model is configured with five one-way self-nested grids with grid-spacings of 108, 36, 12, 4 and 3 km. The 3-km mesh have 35 layers (18 below 1500 m) in the vertical, with the model top at 23 km. The lowest "thermodynamic" level is located at 5.3 meters above the model ground, while the lowest "momentum" level is located at 10.6 meters.

The Eta model analysis at 90.75 km grid-spacing from NCEP is used as the upper-air analysis. The Eta analysis is available on 38 pressure levels from 5.0 to 100.0 kPa every 2.5 kPa. To obtain an upper-air analysis on terrain-following MC2 3-km model levels, the Eta analysis is interpolated horizontally to 108 km, and vertically to MC2 108-km model levels. MC2 108-km driven by the interpolated Eta analysis and forecasts is integrated 1 h. The 0 h and 1 h output from MC2 108-km are used as initial and boundary conditions to drive MC2 36 km, which in turn drive 12, 4, and 3 km. MC2 3 km output on terrain-following levels at 0 h is an upper-air analysis used below. By doing this, horizontal interpolation is gradual from coarse grid to finer grids and vertical interpolations are done on terrain-following coordinate except the one from Eta analysis (pressure levels) to MC2 108-km model levels. Therefore, interpolation errors are minimized.

Now we have a surface data analysis, an upper-air analysis, and the 3D first-guess from previous 3-km run. The three sources of data are on MC2 3-km model levels. Two schemes are proposed below to combine the three data sources to form a final analysis to initialize MC2 3-km assimilation runs.

Scheme I (SIGM) uses a sigmoidal function to influence the background above the lowest model level by the analysis increments at the lowest model level. The scheme assumes that the analysis increments at the lowest model level apply to the whole BL, considering probably similar forecast errors in the BL. Above the BL top, the final analysis is a weighted average of only the first-guess and the upper-air analysis. The weights depend on the ratio of error variance of upper-air analysis and the background. As the upper-air analysis is obtained by interpolating the Eta analysis to the MC2 3-km model level, we assume that the error variance is the same for both the background and upper-air analysis. A transition zone exists near the BL top. The BL height in this scheme is diagnosed by the Stull's transilient turbulence theory (TTT) mixing potential approach.

In the scheme II (PROF) profile method, potential temperatures at the lowest model level are assumed to be mixed uniformly within the BL, so the potential temperature analysis at the lowest model level is applied to the whole BL. Above the BL top, the final analysis is a weighted average of the first-guess and upper-air analy-

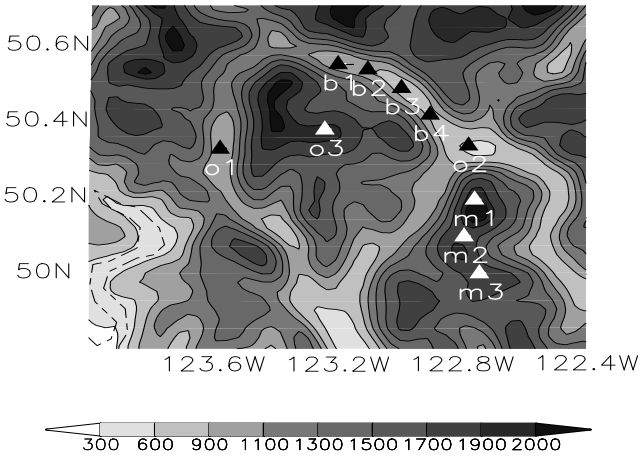

Figure 3: Virtual surface observation stations, indicated by solid triangles, used in the analysis and verification. The stations are positioned at the truth-model terrain height in the Coast Mountains north of Vancouver. Station o1 (50.326 °N, 123.578 °W) is near the mouth of the Elaho River, on the valley floor. Station o2 (50.3344 °N, 122.767 °W) is near the town of Pemberton, also in a valley. Station o3 (50.3773 °N, 123.2363 °W) is at the mountain top. Terrain elevations are from the truth model in meters. Darker shading indicates higher elevations, with a maximum elevation difference of 2055 m in this figure.

sis as in SIGM. BL height is diagnosed from a profile method (described below) based on a slab idealization of the mixed layer (Stull 2000). A jump of potential temperature at the entrainment zone is taken as 1.5 K.

In the profile method, the analyzed potential temperature at the lowest model level $\theta^{SA}(1)$ is compared with the potential temperature profile of the upper-air analysis (θ^{UA}) at successively higher grid points. When $\theta^{SA}(1) - \theta^{UA}(1) > -1.5$ K, the BL height Z_i is the height of the model level k at which the criterion of $\theta^{UA}(k) - \theta^{SA}(1) \geq 1.5$ K is first met. When $\theta^{SA}(1) - \theta^{UA}(1) \leq -1.5$ K, Z_i is assumed to be 300 m, which represents nocturnal BLs or shallow BLs with cold air pooling.

Once the final analysis is obtained as proposed above, incremental analysis updating (IAU, similar to Bloom et al. 1996) is used to insert the final analysis increments (the difference between the final analysis and the first-guess) into the MC2 model. The IAU is implemented for the MC2 model in a similar way to the one in the Advanced Regional Prediction System (ARPS), which assimilates the ADAS analysis increments.

Table 1: Analysis experiments performed. R_h and R_z are correlation length scales in the horizontal and vertical, respectively, which define the regions of influence. d_{ij} and Δz_{ij} are straight-line horizontal distance and elevation difference between an analysis grid point (GP) and the observation station, respectively. K_z is a coefficient. s_{ij} is the circuitous travel distance from the observation to an analysis GP determined in the mother-daughter program. S_{od} is the sharing factor at an analysis GP, which represents how much the analysis GP shares the observation information. S_{od}^{MT} is the same as S_{od} except that the former is from the refined mother-daughter approach. In this study, R_h is 90 km for the first and second iteration, 60 km for the third iteration, 30 km for the fourth and fifth iteration, during the ADAS assimilation cycle.

Experiment	**Correlation function (ρ)**
GAUSS	$\exp(-\frac{1}{2}\frac{\lvert d_{ij}\rvert^2}{R_h^2}) \cdot \exp(-\frac{1}{2}\frac{\lvert \Delta z_{ij}\rvert^2}{R_z^2})$
TERR_DIFF	$\exp(-\frac{1}{2}\frac{\lvert d_{ij}\rvert^2}{R_h^2}) / (1 + K_z \cdot \lvert \Delta z_{ij}\rvert^2)$
MD	$\exp(-\frac{1}{2}\frac{s_{ij}^2}{R_h^2}) \cdot S_{od}$
MD_MT	$\exp(-\frac{1}{2}\frac{s_{ij}^2}{R_h^2}) \cdot S_{od}^{MT}$

4. NUMERICAL RESULTS

4.1 Surface Data Analysis

4.1.1 Virtual observations

We first use "fraternal-twin" experiments to evaluate the MD approach after the mountain-top refinement for the same case (7-8 March 2003) in Deng and Stull (2004). In the fraternal-twin experiments, the "truth" model (MC2 at 2 km grid-spacing) is integrated 12 h to generate a reference atmosphere, from which virtual surface observations are extracted. The "analysis" model (MC2 at 3 km grid-spacing) is started from the same but randomly perturbed initialization conditions and is integrated 12 h to provide a first-guess.

Table 2 lists the normalized root mean square errors

Table 2: The normalized root mean square errors (NRMSE) between the analyses and observations for different sets of the verification stations. One set is the valley stations (b1, b2, b3 and b4); the other is the mountain-top stations (m1, m2 and m3). The analyses were produced when the single mountain-top observation o3 only is used. The observation stations are shown in Fig. 3. NRMSE is RMSE (root mean square error) for each experiment normalized by the RMSE of the first-guess (FSTG). Smaller NRMSE corresponds to better analyses. NRMSE close to 1.0 indicates very small correction to the first-guess from the observations.

EXP	**Verified against b1, b2, b3 and b4**	**Verified against m1, m2 and m3**
FSTG	1.0	1.0
GAUSS	1.1025	0.2745
TERR_DIFF	1.4061	0.2143
MD	1.0009	1.0
MD_MT	1.0026	0.1633

Table 3: Same as Table 2, but for all of the verification stations (the valley stations b1, b2, b3 and b4, and the mountain-top stations m1, m2 and m3). The analyses were produced using two observations (o1 and o2) in different valleys and one mountain-top observation o3.

EXP	**Verified against b1, b2, b3, b4, m1, m2 and m3**
FSTG	1.0
GAUSS	1.7593
TERR_DIFF	1.9668
MD	0.9720
MD_MT	0.4147

(NRMSEs) between different sets of the virtual surface observations (see Fig. 3) and the analyses from different experiments, when the single mountain-top observation o3 only is used to produce an analysis. The observation increment is -1.56 K. The experiments GAUSS, TERR_DIFF and MD are the same as in Deng and Stull (2004). They differ from each other in the definition of background-error correlation (see Table 1). Experiment MD_MT is the same as experiment MD except that the SFs come from the MD approach after mountain-top refinement. The second column in Table 2 indicates that experiment MD and MD_MT produce almost zero spread from the mountain-top observation into valleys as expected. As shown in the third column, experiment GAUSS and TERR_DIFF reduce RMSEs largely from the first-guess by spreading the observation increments into surrounding high mountains. Experiment MD produces identical RMSE as the first-guess (FSTG). While allowing spread into the surrounding high ridges, experiment MD_MT reduces the NRMSE from 1.0 to 0.1633, compared to experiment MD.

Table 3 lists the verification summary when the three observations (two valley observations o1 and o2, and one mountain-top observation o3) are used to produce an analysis. The verification is done for independent valley observations (b1, b2, b3 and b4) and mountain-top observations (m1, m2 and m3) shown in Fig. 3. Overall, experiment MD_MT has minimum NRMSE.

4.1.2 Real observations

Experiments are conducted for the 29-30 July 2003 case when a large wild forest fire occurred in McClure, BC. The weather situation during 29-30 July 2003 was characterized by a strong ridge over Southern BC. Surface analyses are performed at 00 UTC 30 July, by blending hourly surface observations with the first-guess at the lowest terrain-following model level valid at the same time. The analysis domain is shown in Fig. 2. Surface observations are from several agencies: BC ministry of Transportation and Highways (MOTH), BC Ministry of Water Land and Air Protection (WLAP), BC Ministry of Forests (MOFS), CN Railroad (CNRL), CP Rail (CPRL), Environment Canada (EC) and BC Hydro (HYDR). Those surface stations with the difference between their elevation and model topography greater than 500 m are excluded from analysis and verification. Observations separated by 100 m or less in the horizontal and vertical are averaged to create a smaller number of "superobservations".

The verification statistics (Table 4) show that all schemes improve FSTG as measured by bias, mean absolute error (MAE) and normalized root mean square error (NRMSE). GAUSS is slightly better than

Table 4: Verification of analyzed potential temperatures in terms of bias, mean absolute error (MAE), and normalized root mean square error (NRMSE) for all reporting verification stations at the analysis time: 00 UTC 30 July, 2003. N equals total number of reporting stations. NRMSE is RMSE (root mean square error) for each experiment normalized by the RMSE of the first-guess (FSTG).

EXP	**N**	**Bias (K)**	**MAE(K)**	**NRMSE**
FSTG	64	-5.2583	7.6869	1.
GAUSS	64	0.7577	2.0990	0.5146
TERR_DIFF	64	0.7121	2.3238	0.5462
MD	64	0.0894	1.5997	0.3906
MD_MT	64	0.1332	1.6102	0.3872

TERR_DIFF, with smaller MAE and NRMSE. Both MD and MD_MT outperform GAUSS and TERR_DIFF. MD produces lowest bias, MAE, whereas MD_MT has lowest NRMSE. The improvement of MD_MT over MD is not as obvious as that for the virtual observation case in the previous subsection.

4.2 Data Assimilation Results

To assess the impacts of the different schemes on subsequent forecasts, six experiments are examined: one control experiment without assimilation (CTRL) and five other experiments, which assimilate various combinations of the surface data analysis and upper-air analysis (see Table 5). Experiment SIGMDA uses the surface analysis increments within the BL and the upper-air analysis increments above BL, where two analysis increments are combined by scheme SIGM described above. Experiment PROFDA uses the surface analysis and upper-air analysis combined by scheme PROF. These two experiments are performed to see which combination scheme is better for subsequent forecasts. Experiment SURFDA uses the surface data analysis only at the lowest model level, above which are the first-guess. This experiment is used to study the effect of assimilating surface observations at only one model level. Experiment SF_SIGM uses the surface analysis only, but the analysis increments at the lowest model level are spread by scheme SIGM to the whole BL. Experiment SF_PROF is the same as SF_SIGM, except that the surface analysis is spread vertically by PROF. These two experiments are conducted to see if the surface data assimilation plays a dominant role on subsequent surface forecasts.

A schematic illustrating the assimilation and forecast periods is shown in Fig. 4. All assimilation runs are started at 00 UTC on day 2 and are integrated 24 h. Experiment CTRL is started at 12 UTC on day 1 and is integrated 36 h. CTRL provides its 12 h output as the first-guess for analysis at 00 UTC on day 2. Surface observations and Eta analysis valid at 00 UTC on day 2 are used to produce a new analysis. Verification of subsequent forecasts at the lowest model level is performed during a 24 h forecast period from 00 UTC on day 2 to 00 UTC on day 3.

All DA experiments assimilate only temperature observations from the surface analysis and/or upper-air analysis for the 29-30 July 2003 case. For fair-comparison purposes, upper-air analyses are used at the grid-points where the absolute values of the temperature analysis increments at the lowest model level are greater than 1.0E-03 K. For all experiments, surface analyses are from MD_MT; the final analysis increments are incorporated all at once by IAU within a 30 seconds (one time step) window. The subsequent forecasts at the lowest model level are verified against surface observations. Bias, MAE and RMSE between observations and forecasts are calculated.

Statistical assessments during 1-12 h forecast period in Table 6 suggest that different experiments have variable success at predicting surface fields. For temperature forecasts, all of the DA experiments outperform CTRL. By assimilating surface temperature only at the lowest model level, experiment SURFDA gives very little improvement over CTRL. When surface potential temperature analyses from MD_MT are spread throughout the whole BL either through SIGM or PROF, larger improvement for predicting surface temperatures are achieved. The two experiments (SIGMDA and PROFDA) that combine the surface and upper-air analysis gain larger improvement over CTRL than any other experiments that assimilate surface data only. The difference in the error measures between SIGMDA and PROFDA is very small.

For SLP forecasts, all DA experiments also outperform CTRL except SURFDA. Overall, improvement of SLP forecasts is smaller than the one of temperature forecasts. This is reasonable as temperature is directly assimilated into the model. For wind forecasts, all DA experiments underperform CTRL in terms of normalized root mean square vector error (NRMSVE) due to initial

Table 5: Experiment design to test different schemes combining surface data analysis and upper-air analysis.

EXP Name	Surface Analysis	Upper-air Analysis	Combination Scheme
CTRL	No	No	
SIGMDA	Yes	Yes	SIGM
PROFDA	Yes	Yes	PROF
SURFDA	Yes	No	
SF_SIGM	Yes	No	SIGM
SF_PROF	Yes	No	PROF

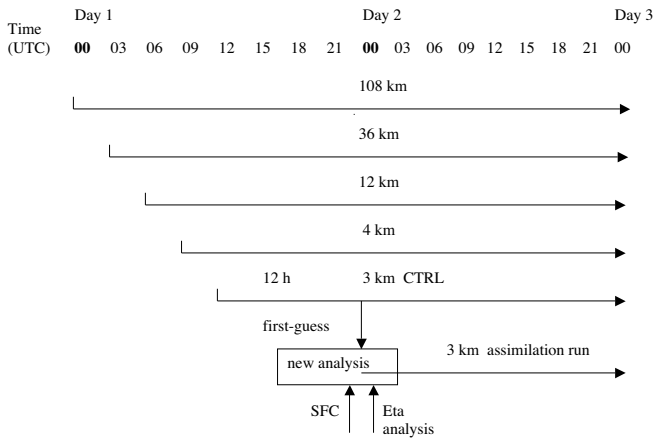

Figure 4: Schematic diagram illustrating time-lines of MC2 self-nested grids, 3-km CTRL run and 3-km assimilation runs. MC2 4-km provides boundary conditions for 3-km CTRL run and 3-km assimilation runs. SFC indicates surface data.

Table 6: Verification of surface potential temperatures (θ), wind (**V**) and mean sea level pressure (SLP) forecasts in terms of bias, mean absolute error (MAE), root mean square error (RMSE) and/or normalized RMSE (NRMSE) for all reporting verification stations (n) during 12 h forecast period from 01 UTC 30 to 12 UTC 30 July, 2003. NRMSE is RMSE for each experiment normalized by the RMSE of the control run (CTRL).

	1 - 12 h								
	θ (K) (n = 601)				SLP (hPa) (n = 153)			**V** (m s-1) (n = 506)	
Experiment	**BIAS**	**MAE**	**RMSE**	**NRMSE**	**BIAS**	**MAE**	**NRMSE**	**RMSVE**	**NRMSVE**
CTRL	-4.8380	5.6661	6.4715	1.	3.7556	3.9732	1.	1.7445	1.
SIGMDA	-4.1647	5.1123	5.9504	0.9195	3.1126	3.5925	0.9329	1.9478	1.1165
PROFDA	-4.1629	5.1785	5.9788	0.9239	3.0049	3.5659	0.9348	1.9958	1.1441
SURFDA	-4.8528	5.6228	6.4421	0.9955	3.7572	3.9703	1.0003	1.7502	1.0033
SF_SIGM	-4.3195	5.2334	6.0702	0.9380	3.2345	3.6122	0.9368	1.9604	1.1238
SF_PROF	-4.3279	5.2882	6.0890	0.9409	3.2109	3.6500	0.95511	1.9682	1.1282

imbalance between mass and wind fields after assimilating temperatures. SURFDA has the smallest NRMSVE, probably because the assimilated temperature information is soon lost after insertion, whereas PROFDA has the largest NRMSVE. The differences between NRMSVEs of different experiments are small.

Verification statistics for 13-24 h forecast period (not shown) indicates that all assimilation experiments produce temperature, wind and SLP forecasts that are closer to those from CTRL.

Experiments are conducted to assess different data assimilation strategies. Experiment TH1 incorporates temperature analysis increments all at once within a 30 seconds data assimilation window. In experiment TH3, the temperature analysis increments are incorporated every 120 seconds over a 1 h data assimilation window. The 1 h window is selected based on the fact that BL responds to the surface forcing with a time scale of about one hour or less (Stull 1988). In experiment TH6, the temperature analysis increments are incorporated every 1200 seconds over a 1 h window. For all these three experiments, the final analysis is obtained through PROF scheme. Therefore, experiment TH1 is identical to PROFDA in table 6.

Fig. 5 shows NRMSE of potential temperature versus forecast hours for experiment TH1, TH3 and TH6. The NRMSEs for these experiments is smaller than 1.0 during the first 12 h (except 4 h) forecasts, and increase

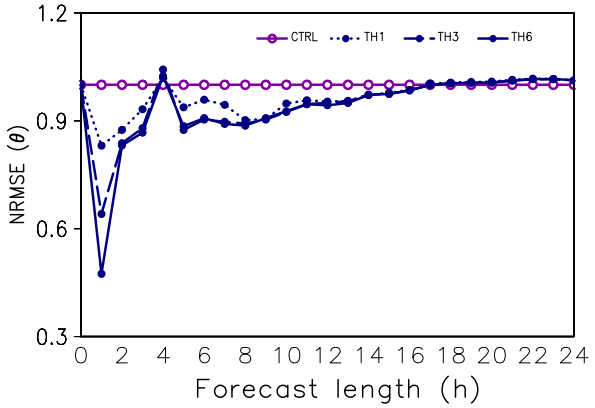

Figure 5: Time series of normalized root mean square error (NRMSE) for surface potential-temperature from experiment CTRL, TH1, TH3, and TH6.

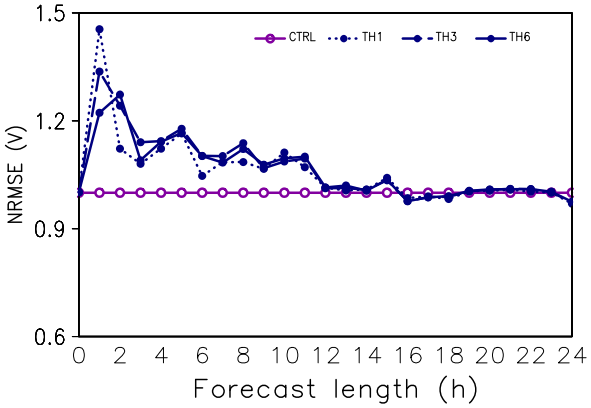

Figure 6: Time series of normalized root mean square vector error (NRMSVE) for surface winds from experiment CTRL, TH1, TH3, and TH6.

gradually with forecast hours. Finally the NRMSE becomes closer to 1.0. By applying the analysis increments over a 1 h window rather than all at once, experiment TH3 and TH6 produce much smaller NRMSE than experiment TH1 for the first 7 h (except 4 h) forecast. Reducing the rate at which data are assimilated decreases NRMSE for the 1 h forecast.

The evolution of NRMSVE for experiment TH1, TH3 and TH6 is shown in Fig. 6. By assimilating temperatures only, the model tends to produce poorer wind forecasts during the first 12 h, due to initial imbalances between the mass and wind fields. During the second 12 h forecast period, all DA experiments and CTRL produce similar results. This could be because the assimilated information propagate out of the domain. Another reason could be that the mass and wind fields are adjusted to be in balance. By applying the temperature analysis increments over a 1 h window rather than all at once (thus reducing initial imbalances), experiment TH3 and TH6 decrease NRMSVE effectively for the 1 h forecast as compared to experiment TH1, but increase NRMSVE a little bit during the 2-8 h forecast period. Reducing the rate at which data are assimilated decreases further NRMSVE for the 1 h forecast while reducing the increase of NRMSVE.

5. Summary

A mountain-top refinement is introduced to the original mother-daughter (MD) approach (Deng and Stull 2004), and is tested with two cases. The MD approach after mountain-top refinement (MD_MT) has larger improvement over MD for the virtual observation case than for the real observation case. A reason for this performance could be that only a very small fraction of stations (three out of the 64 stations) are treated as mountain-top observations in the real observation case, while in the virtual observation case, one out of the three stations is a mountain-top observation.

By assimilating temperature observations only, the model improves surface temperature and mean sea level pressure forecasts during the first 12 h, but tends to produce poorer forecasts of surface winds due to the initial imbalance. Surface information assimilated only at the lowest model level is soon lost at the beginning of the forecast period. Larger improvement over the control run is achieved when surface information is spread upward throughout the BL. Experiments that spread surface information by the two combination schemes (SIGM and PROF) behave only slightly differently.

By applying the temperature analysis increments over a 1 h window rather than all at once by using incremental analysis update (IAU), the model decreases effectively NRMSE of potential temperature for the first 7 h forecast (and NRMSVE of winds for the first 1 h forecast). The IAU over a proper data assimilation window can reduce initial imbalances, but can't remove initial imbalances completely if temperature data only are assimilated.

REFERENCES

Alapaty, K., N. L. Seaman, D. S. Niyogi, and A. F. Hanna, 2001: Assimilating surface data to improve the accuracy of atmospheric boundary layer simulations. *J. Appl. Meteor.*, **40**, 2068–2082.

Bloom, S. C., L. L. Takacs, A. M. da Silva, and D. Ledv-

ina, 1996: Data assimilation using incremental analysis updates. *Mon. Wea. Rev.*, **124**, 1256–1271.

Bratseth, A. M., 1986: Statistical interpolation by means of successive corrections. *Tellus*, **38A**, 439–447.

Brewster, K., 1996: Application of a Bratseth analysis scheme including Doppler radar data. Preprints, *15th Conf. on Weather Analysis and Forecasting*, AMS, Boston, 92–95.

Daley, R., 1991: *Atmospheric data analysis*. Cambridge Atmospheric and Space Science Series, Cambridge University Press, Cambridge, 457 pp.

Deng, X. X. and R. Stull, 2004: A mesoscale analysis method for surface potential temperature in mountainous and coastal terrain. *Mon. Wea. Rev.*, **Accepted**.

Kalnay, E., 2003: *Atmospheric Modeling, Data Assimilation and Predictability*. Cambridge University Press, Cambridge, 341 pp.

Miller, P. A. and S. G. Benjamin, 1992: A system for the hourly assimilation of surface observations in mountainous and flat terrain. *Mon. Wea. Rev.*, **120**, 2342–2359.

Ruggiero, F. H., K. D. Sashegyi, R. V. Madala, and S. Raman, 1996: The use of surface observations in four-dimensional data assimilation using a mesoscale model. *Mon. Wea. Rev.*, **124**, 1018–1033.

Stull, R. B., 1988: *An Introduction to Boundary Layer Meteorology*. Kluwer Academic Press, P.O. Box 17, 3300 AA Dordrecht, The Netherlands, 666 pp.

— 2000: *Meteorology for Scientists and Engineers*. Brools/Cole Thomson Learning, 511 Forest Lodge Road, Pacific Grove, CA 93950 USA, 2nd edition, 502 pp.